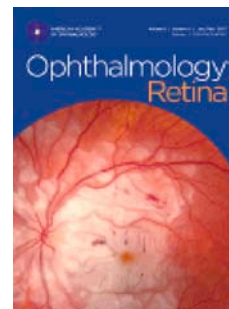


Journal Pre-proof



The Natural History of Leber Congenital Amaurosis and Cone-Rod Dystrophy Associated with Variants in the *GUCY2D* Gene

Leo C. Hahn, MD, Michalis Georgiou, MD, PhD, Hind Almushattat, BAS, Mary J. van Schooneveld, MD, PhD, Emanuel R. de Carvalho, MD, PhD, Nieneke L. Wesseling, MD, Jacqueline B. ten Brink, BAS, Ralph J. Florijn, PhD, Birgit I. Lissenberg-Witte, PhD, Ine Strubbe, MD, Caroline van Cauwenbergh, PhD, Julie de Zaeytijd, MD, Sophie Walraedt, MD, Elfride de Baere, MD, PhD, Rajarshi Mukherjee, MD, Martin McKibbin, MD, Magda A. Meester-Smoor, PhD, Alberta A.H.J. Thiadens, MD, PhD, Saoud Al-Khuzaei, MD, Engin Akyol, MD, Andrew J. Lotery, MD, Maria M. van Genderen, MD, PhD, Jeannette Ossewaarde-van Norel, MD, PhD, L. Ingeborgh van den Born, MD, PhD, Carel B. Hoyng, MD, PhD, Caroline C.W. Klaver, MD, PhD, Susan M. Downes, MBChB, MD(R), Arthur A. Bergen, PhD, Bart P. Leroy, MD, PhD, Michel Michaelides, MD (Res), FRCOphth, Camiel J.F. Boon, MD, PhD

PII: S2468-6530(22)00107-5

DOI: <https://doi.org/10.1016/j.oret.2022.03.008>

Reference: ORET 1189

To appear in: *Ophthalmology Retina*

Received Date: 22 November 2021

Revised Date: 20 February 2022

Accepted Date: 14 March 2022

Please cite this article as: Hahn L.C., Georgiou M., Almushattat H., van Schooneveld M.J., de Carvalho E.R., Wesseling N.L., ten Brink J.B., Florijn R.J., Lissenberg-Witte B.I., Strubbe I., van Cauwenbergh C., de Zaeytijd J., Walraedt S., de Baere E., Mukherjee R., McKibbin M., Meester-Smoor M.A., Thiadens A.A.H.J., Al-Khuzaei S., Akyol E., Lotery A.J., van Genderen M.M., Ossewaarde-van Norel J., van den Born L.I., Hoyng C.B., Klaver C.C.W., Downes S.M., Bergen A.A., Leroy B.P., Michaelides M. & Boon C.J.F., The Natural History of Leber Congenital Amaurosis and Cone-Rod Dystrophy Associated with Variants in the *GUCY2D* Gene, *Ophthalmology Retina* (2022), doi: <https://doi.org/10.1016/j.oret.2022.03.008>.

This is a PDF file of an article that has undergone enhancements after acceptance, such as the addition of a cover page and metadata, and formatting for readability, but it is not yet the definitive version of record. This version will undergo additional copyediting, typesetting and review before it is published in its final form, but we are providing this version to give early visibility of the article. Please note that, during the production process, errors may be discovered which could affect the content, and all legal disclaimers that apply to the journal pertain.

© 2022 by the American Academy of Ophthalmology Published by Elsevier Inc.

1 **The Natural History of Leber Congenital Amaurosis and Cone-Rod Dystrophy**
2 **Associated with Variants in the *GUCY2D* Gene**

3
4 Leo C. Hahn, MD¹; Michalis Georgiou, MD, PhD²; Hind Almushattat, BAS¹; Mary J. van
5 Schooneveld, MD, PhD^{1,3}; Emanuel R. de Carvalho, MD, PhD²; Nieneke L. Wesseling,
6 MD¹; Jacqueline B. ten Brink, BAS⁴; Ralph J. Florijn, PhD⁴; Birgit I. Lissenberg-Witte, PhD⁵;
7 Ine Strubbe, MD⁶; Caroline van Cauwenbergh, PhD^{6,7}; Julie de Zaeytijd, MD⁶; Sophie
8 Walraedt, MD⁶; Elfride de Baere, MD, PhD^{6,7}; Rajarshi Mukherjee, MD⁸; Martin McKibbin,
9 MD⁸; Magda A. Meester-Smoor, PhD⁹; Alberta A.H.J. Thiadens, MD, PhD⁹; Saoud Al-
10 Khuzaei, MD¹⁰; Engin Akyol, MD¹¹; Andrew J. Lotery, MD¹¹; Maria M. van Genderen, MD,
11 PhD^{3,12}; Jeannette Ossewaarde-van Norel, MD, PhD¹²; L. Ingeborgh van den Born, MD,
12 PhD¹³; Carel B. Hoyng, MD, PhD¹⁴; Caroline C.W. Klaver, MD, PhD^{9,14}; Susan M. Downes,
13 MBChB, MD(R)¹⁰; Arthur A. Bergen, PhD^{4,15}; Bart P. Leroy, MD, PhD^{6,7,16};
14 Michel Michaelides, MD (Res), FRCOphth^{2,17}; Camiel J.F. Boon, MD, PhD^{1,18}

15
16 **Authors affiliations**

- 17 1. Department of Ophthalmology, Amsterdam University Medical Centers, University of
18 Amsterdam, Amsterdam, The Netherlands
19 2. Moorfields Eye Hospital NHS Foundation Trust, London, United Kingdom
20 3. Bartiméus, Diagnostic Center for Complex Visual Disorders, Zeist, The Netherlands
21 4. Department of Clinical Genetics, Amsterdam University Medical Centers, University of
22 Amsterdam, Amsterdam, The Netherlands
23 5. Department of Epidemiology and Data Science, Amsterdam University Medical Centers,
24 Vrije Universiteit Amsterdam, Amsterdam, The Netherlands
25 6. Department of Ophthalmology, Ghent University Hospital, Ghent University, Ghent,
26 Belgium
27 7. Center for Medical Genetics Ghent, Ghent University Hospital & Ghent University, Ghent,
28 Belgium
29 8. Department of Ophthalmology, St James's University Hospital, Leeds, United Kingdom
30 9. Department of Ophthalmology, Erasmus Medical Center, Rotterdam, The Netherlands
31 10. Oxford Eye Hospital, John Radcliffe Hospital, Oxford University Hospitals NHS
32 Foundation Trust, & Nuffield Laboratory of Ophthalmology, University of Oxford, Oxford,
33 United Kingdom
34 11. Eye Unit, University Hospital Southampton, Southampton, United Kingdom
35 12. Department of Ophthalmology, University Medical Center Utrecht, Utrecht, Netherlands
36 13. The Rotterdam Eye Hospital and the Rotterdam Ophthalmic Institute, Rotterdam, The
37 Netherlands
38 14. Department of Ophthalmology, Radboud University Medical Center, Nijmegen, The
39 Netherlands
40 15. The Netherlands Institute for Neuroscience (NIN-KNAW), Amsterdam, The Netherlands
41 16. Division of Ophthalmology and Center for Cellular and Molecular Therapeutics,
42 Children's Hospital of Philadelphia, Philadelphia, United States of America
43 17. UCL Institute of Ophthalmology, University College London, London, United Kingdom
44 18. Department of Ophthalmology, Leiden University Medical Center, Leiden, The
45 Netherlands

46
47 **Address correspondence to:**

48 Camiel J.F. Boon, MD, PhD, FEBO
49 Amsterdam University Medical Centers
50 PO Box 22660
51 1100 DD Amsterdam
52 The Netherlands
53 Email: Camiel.boon@amsterdamumc.nl
54

55 **Meeting presentations:**

56 Annual meeting of the Netherlands Ophthalmological Society, 2021
57 Annual meeting of the Association for Research in Vision and Ophthalmology, 2021
58 Annual meeting of the European Society of Retina Specialists, 2021
59

60 **Funding and Support:**

61 This research was primarily supported by the ODAS foundation (grant 2018-2 [C.J.F.B]) and
62 the European Society of Retina Specialists (EURETINA Clinical Research Award 2019, grant
63 2019-1974 [L.C.H., C.J.F.B]).

64 The collection of data in the participating centers was partially supported by the Ghent
65 University Special Research Fund (BOF15/GOA/011 to E.D.B. and BOF20/GOA/023 to
66 E.D.B. and B.P.L.) and by the Ghent University Hospital Innovation Fund (NucleUZ to
67 E.D.B.). E.D.B. (1802220N) and B.P.L. (1803821N) are Senior Clinical Investigators of the
68 Fonds voor Wetenschappelijk Onderzoek. Furthermore, this work has also been supported by
69 grants from the National Institute for Health Research Biomedical Research Centre at
70 Moorfields Eye Hospital NHS Foundation Trust and UCL Institute of Ophthalmology,
71 Moorfields Eye Charity, and Retina UK. The Oxford EYE Hospital was supported by the
72 Oxfordshire and South Midlands Clinical research Network and the UK Inherited Retinal
73 Dystrophy Consortium Project (Retina UK, GR586). The views expressed are those of the
74 authors and not necessarily those of the NHS, the NIHR or the Department of Health. Saoud
75 Al-Khuzaei is supported by a scholarship from the Qatar National Research Fund (GSRA6-1-
76 0329-19010). The RD5000 consortium was supported by Uitzicht (grant 2015-30 financed by
77 ODAS, Oogfonds, Retinafonds and Bartiméus Sonneheerdt).

78 This study was performed as part of a collaboration within the Dutch RD5000 network for
79 rare retinal dystrophies, and European Reference Network for Rare Eye Diseases (ERN-
80 EYE). E.D.B., C.C.W.K., L.I.v.d.B., C.B.H, B.P.L., A.A.B. & C.J.F.B. are members of ERN-
81 EYE, which is co-funded by the Health Program of the European Union under the Framework
82 Partnership Agreement No 739534 'ERN-EYE'. The sponsors, funding or collaborating
83 organizations had no role in the design or conduct of this research.

84 **Conflict of Interest:** no conflicting relationship exists for any author.

85 **Running head:** Leber Congenital Amaurosis and Cone-Rod Dystrophy Associated with
86 *GUCY2D*

87
88 **Address for reprints:**

89 Camiel J.F. Boon, MD, PhD, FEBO
90 Amsterdam University Medical Centers
91 PO Box 22660
92 1100 DD Amsterdam
93 The Netherlands

94 Email: Camiel.boon@amsterdamumc.nl

95

96 This article contains additional online-only material. The following should appear online-
97 only: Supplemental Figures 1, 2 and Supplemental Tables 1, 2, 3, 4.

Journal Pre-proof

98 **Abstract**

99 **Objective**

100 To describe the spectrum of Leber congenital amaurosis (LCA) and cone-rod dystrophy
101 (CORD) associated with the *GUCY2D* gene, and to identify potential clinical endpoints and
102 optimal patient selection for future therapeutic trials.

103 **Design**

104 International multicenter retrospective cohort study.

105 **Subjects**

106 82 patients with *GUCY2D*-associated CORD and LCA from 54 molecularly confirmed
107 families.

108 **Methods**

109 Data were gathered by reviewing medical records for medical history, symptoms, best-
110 corrected visual acuity (BCVA), ophthalmoscopy, visual fields, full-field electroretinography
111 and retinal imaging (fundus photography, spectral-domain optical coherence tomography
112 (SD-OCT), fundus autofluorescence).

113 **Main Outcomes Measures**

114 Age of onset, annual decline of visual acuity, estimated visual impairment per age, genotype-
115 phenotype correlations, anatomic characteristics on funduscopy, and multimodal imaging.

116 **Results**

117 Fourteen patients with autosomal recessive LCA and 68 with autosomal dominant CORD
118 were included. The median follow-up time was 5.2 years (interquartile range (IQR), 2.6-8.8)
119 for LCA, and 7.2 years (IQR, 2.2-14.2) for CORD. Generally, LCA presented in the first year
120 of life. The BCVA in LCA ranged from no light perception to 1.00 logMAR, and remained
121 relatively stable during follow-up. Imaging for LCA was limited, but showed little to no

122 structural degeneration. In *CORD*, progressive vision loss started around the second decade of
123 life. The annual decline rate of visual acuity was 0.022 logMAR ($P < 0.001$), which did not
124 differ between the c.2513G>A and the c.2512C>T *GUCY2D* variant ($P = 0.798$). At the age
125 of 40 years the probability of being blind or severely visually impaired was 32%. The
126 integrity of the ellipsoid zone (EZ) and external limiting membrane (ELM) on SD-OCT were
127 correlated significantly with BCVA (Spearman's $\rho = 0.744$, $P = 0.001$ and $\rho = 0.712$, $P <$
128 0.001 , respectively) in *CORD*.

129 **Conclusion**

130 LCA due to variants in *GUCY2D* results in severe congenital visual impairment with
131 relatively intact macular anatomy on funduscopy and available imaging, suggesting a long
132 preservation of photoreceptors. Despite large variability, *GUCY2D*-associated *CORD*
133 generally presented during adolescence with a progressive loss of vision and culminated in
134 severe visual impairment during mid to late-adulthood. The integrity of the ELM and EZ may
135 be suitable structural endpoints for therapeutic studies in *GUCY2D*-associated *CORD*.

136 INTRODUCTION

137 Leber congenital amaurosis (LCA) and Cone-rod dystrophy (CORD) are relatively common
138 inherited retinal dystrophies (IRDs), which frequently lead to significant visual impairment in
139 young patients.¹⁻³ Typically, LCA causes severe congenital visual impairment or blindness
140 with absent to minimal residual electroretinography (ERG) responses, often in combination
141 with nystagmus, photophobia, and eye poking.^{2,4} Patients with CORD tend to present with
142 mild to moderate loss of visual acuity and/or color vision disturbance within the first decades
143 of life, which generally progresses to severe visual impairment or even legal blindness during
144 adulthood.^{5,6} One of the most common genes causing these conditions is the *GUCY2D* gene,
145 which has been found to be responsible for up to 20% of all LCA, and up to 25% of all
146 autosomal dominant CORD cases.^{3,4}

147 The *GUCY2D* gene encodes the enzyme retinal guanylate cyclase 1, which plays a crucial role
148 in photoreceptors recovery to the dark-adapted state by regulating intracellular Ca^{2+}
149 concentration.⁷ Currently, there is no treatment available for patients with IRDs associated
150 with *GUCY2D*. However, for *GUCY2D*-associated LCA improvements in electrophysiology
151 and visual function were seen after experimental gene replacement therapy in animal and
152 preliminary human phase I/II studies.^{8,9}

153 Interestingly, the great majority of patients with CORD associated with *GUCY2D* have
154 disease-causing variants in codon 838, out of which up to 87% are the two most prevalent
155 variants described in the current study.¹⁰ The high prevalence of these variants and their
156 proximity to each other make them attractive potential targets for gene editing approaches. In
157 animal models CRISPR/Cas9 was successfully used to knockout *GUCY2D* expression, which
158 may be a viable first step towards a therapeutic approach for *GUCY2D*-associated CORD.¹¹

159 To select the most appropriate design for human gene therapy trials, as well as the most
160 suitable candidates and clinical endpoints for such trials, a thorough understanding of IRDs

161 associated with *GUCY2D* is essential. In addition, patients and clinicians will benefit from
162 such insights to enable more accurate clinical and prognostic information. Therefore, this
163 international multicenter retrospective study aims to deliver a detailed description of the
164 natural course, phenotype and genotype of *GUCY2D*-associated LCA and CORD.

165

166 **METHODS**

167 **Study population and data collection**

168 Patients were collected from the Delleman archive, a large database for inherited eye diseases
169 at the Amsterdam University Medical Centers (Amsterdam, the Netherlands), and various
170 Dutch expertise centers within the RD5000 consortium, a national consortium for IRDs.¹²
171 Data from additional patients were included from the University Hospital Ghent (Ghent,
172 Belgium), as well as 4 academic tertiary referral centers in the United Kingdom (Moorfields
173 Eye Hospital, St James`s University Hospital Leeds, Oxford Eye Hospital, University
174 Hospital Southampton). For inclusion, patients needed either a molecularly confirmed
175 diagnosis, or a typical clinical presentation and an affected first-degree family member with
176 confirmed disease-causing *GUCY2D* variants. This study was approved by the ethics
177 committee of the Erasmus Medical Center and adhered to the tenets of the Declaration of
178 Helsinki. Eighteen CORD patients from 4 families have been described earlier, but substantial
179 new follow-up data are described in this article.¹³⁻¹⁵ Additionally, for 13 of these patients from
180 a large Dutch family the *GUCY2D* gene had not been identified as disease-causing gene in the
181 previous publication from 1992.¹⁵

182 Data collection was performed by standardized review of medical records for medical history,
183 age at onset, symptoms, family history, best-corrected visual acuity (BCVA), refractive error,
184 dilated fundus examination, full-field ERG, Goldmann visual field testing, color vision

185 testing, spectral-domain optical coherence tomography (SD-OCT), fundus autofluorescence
186 (FAF) images, and color fundus photography. Measurements of retinal thickness and
187 evaluation of layer integrity on SD-OCT were performed within a radius of 500 μ m around the
188 foveal center in the Heidelberg Eye Explorer (Heidelberg Engineering, Heidelberg,
189 Germany). The integrity of EZ and ELM were graded as either intact, disrupted or absent by
190 two independent graders (L.C.H., H.A.). The graders were also masked for other image
191 modalities. Weighted Cohen`s kappa analyses was performed and showed a high inter-rater
192 reliability for the integrity of EZ ($\kappa = 0.892\pm 0.03$, $P < 0.001$) as well as for ELM integrity (κ
193 $= 0.918\pm 0.02$, $P < 0.001$). For the 12 cases in which the graders disagreed, a trained expert
194 referee (C.J.F.B.) decided on the subgroup. The autofluorescence patterns on FAF images
195 were described for each patient by a retinal specialist (C.J.F.B.) and the frequencies for each
196 pattern were subsequently reported.

197 **Statistical analysis**

198 For statistical analysis, SPSS version 23.0 (IBM, Corp, Armonk, NY) and the R software
199 environment were used.¹⁶ Categorical data were expressed in proportions. Continuous data
200 were reported in either mean with standard deviation or median with interquartile ranges
201 (IQR). A multistate model was used to estimate the disease progression based on categories of
202 visual impairment, with the R-package msm. The following states were used as defined by
203 World Health Organization based on the better-seeing eye: mild visual impairment ($20/67 \leq$
204 $BCVA < 20/40$), moderate visual impairment ($20/200 \leq BCVA < 20/67$), severe visual
205 impairment ($20/400 \leq BCVA < 20/200$), and blindness ($BCVA < 20/400$).¹⁷ Linear mixed
206 models were applied to analyze the annual decline rate of BCVA using data of both eyes. To
207 account for inter-eye correlation a random intercept was added to the model.¹⁸ For this
208 analysis, the BCVA values were converted to logarithm of the minimum angle of resolution
209 (logMAR). For hand movement a value of 2.7, for light perception 2.8, and for no light

210 perception 2.9 logMAR was used. Asymmetry of BCVA was defined as minimum difference
211 of 0.3 logMAR between the right and left eye at two consecutive visits.¹⁹

212

213 **RESULTS**

214 **Participants**

215 In total, 82 patients from 54 families were included in this study. Fourteen (17.1%) were
216 diagnosed with autosomal recessive LCA and 68 (82.9%) with autosomal dominant CORD.
217 For 65 out of 82 (79.3%) patients, follow-up data were available with a median follow-up
218 time of 5.2 year (IQR: 1.2-10.8) and a mean number of visits of 3.0 (IQR: 2.0-6.5). The
219 clinical characteristics of the cohort per group are presented in Table 1.

220 **Disease onset, reported symptoms and visual acuity**

221 The median age at onset for LCA was 0.3 years with a range of 0.0-2.2 years, and patients
222 presented with congenital severe visual impairment. Nystagmus was reported in 11/14
223 (78.6%) patients, photophobia in 6/14 (42.9%), eye poking in 5/14 (35.7%), and nyctalopia in
224 1/14 (7.1%). Visual acuity data were available for 12/14 (85.7%) patients and ranged from no
225 light perception to 1.0 logMAR (20/200 Snellen equivalent). The visual acuity did not change
226 significantly during follow-up ($P = 0.811$).

227 In CORD, the reported median age at onset was 14.6 years (IQR: 10.0-26.5 years). Patients
228 presented with mild central vision loss and/or color vision disturbances (Table 1). In one
229 Dutch family, extensive color vision testing in 3 young asymptomatic family members
230 revealed a tritan color vision disturbance as first symptom, and loss of visual acuity only
231 started to develop at later age. The BCVA declined with a rate of 0.022 logMAR annually in
232 CORD patients ($P < 0.001$) based on data of both eyes (Fig 1). The probabilities of being in
233 different states of visual impairment based on the better-seeing eye per age are illustrated in

234 Figure 1 and Supplemental Table 1 (available at www.ophtalmologyretina.org). The BCVA
235 between eyes was strongly correlated (Spearman's $\rho = 0.897$, $P < 0.001$). Asymmetry in
236 BCVA between eyes was seen in 1/14 (7.1%) LCA patients and 13/67 (19.4%) CORD
237 patients.

238 **Ophthalmic findings, funduscopy and multimodal imaging**

239 In 3/14 (21.4%) of LCA patients, an abnormal foveal reflex was described in funduscopy
240 reports. Two (14.3%) LCA patients, were reported to have peripheral mottled RPE
241 pigmentation and 1/14 (7.1%) patient with RPE atrophy in the peripheral retina. Bilateral
242 optic disc pallor was found in 1/14 (7.1%) patient. SD-OCT and FAF imaging was available
243 for 8 out 14 (57.1%) LCA subjects, but the imaging quality was variable due to nystagmus,
244 and only 3/14 (21.4%) had macular scans of sufficient quality. These 3 SD-OCT scans
245 showed a remarkably intact retinal structure and photoreceptor layers in the peripheral and
246 central retina (Fig 2). On FAF imaging in 3/8 (37.5%) LCA patients, central autofluorescence
247 was slightly increased, resulting in a lack of normal foveal hypoautofluorescence (Fig 2F).
248 Three LCA patients (21.4%) had complications likely caused by eye poking, which included
249 bilateral keratoconus, disrupted Descemet's membranes, hydrops, leucoma, corneal scars, and
250 cortical cataract. The cortical cataract developed at the age of 6 in the right eye and the patient
251 underwent uncomplicated cataract surgery with intraocular lens insertion one year later. The
252 BCVA before and after surgery was light perception.

253 The most prominent funduscopy findings described in CORD patients included macular RPE
254 atrophy in 16/65 (24.6%), macular RPE alteration in 18/65 (27.7%), macular mottling in
255 20/65 (30.8%), and bull's-eye maculopathy in 6/65 (9.2%) patients, based on the descriptions
256 in the case notes. In the peripheral retina, RPE atrophy was reported in 1/65 patients (1.5%),
257 RPE alterations in 4/65 patients (6.2%) and lattice-like lesions in 1/65 patients (1.5%).
258 Attenuated retinal blood vessels were recorded in 10/65 (15.4%) and cataract in 8/65 CORD

259 patients (12.3%). Myopia was found in 24/35 (68.6%) patients and high myopia (more than -6
260 diopters) in 10/35 (28.5%) patients. Patients with high myopia did not show a more severe
261 annual decrease of BCVA compared to the rest of the cohort ($p = 0.738$).

262 SD-OCT scans were available for 46/68 (67.6%) and FAF images for 45/68 (66.2%) CORD
263 patients. The imaging showed increased central autofluorescence in early stages, which
264 progressed towards macular atrophy and central absence of autofluorescence (Fig 3). All
265 patient had FAF abnormalities. The frequency of FAF patterns found in this cohort together
266 with integrity of EZ and ELM on SD-OCT are displayed in Table 2. One patient had
267 drusenoid hyperautofluorescent dots on FAF (Fig 4D-H). Disruption as well as absence of the
268 foveal EZ and ELM layer correlated strongly with a decrease in BCVA (Spearman's $\rho =$
269 0.744 , $P < 0.001$ and, Spearman's $\rho = 0.712$, $P < 0.001$, respectively). The median central
270 retinal thickness (CRT) was $142.0 \mu\text{m}$ (IQR: $119.5\text{--}189.0 \mu\text{m}$) and annually decreased by 2.7
271 μm ($P < 0.001$). The CRT correlated strongly between eyes (Spearman's $\rho = 0.933$, $P <$
272 0.001), but only showed a moderate negative correlation with BCVA (Spearman's $\rho = -0.551$,
273 $P < 0.001$). Correlation plots regarding the CRT and integrity of the EZ and ELM are
274 displayed in Supplemental Figure 1 (available at www.opthalmologyretina.org). In 8/46
275 patients (17.4%), an hyporeflective space (optical gap) beneath the macula was seen on SD-
276 OCT at a median age of 49.0 years (range: 21.2-68.0 years; Fig 3D).

277 **Full-field electroretinography and visual fields**

278 ERG findings were recorded in 5/14 (35.7%) patients with LCA, at a median age of 1.4 years
279 (range: 0.2-1.8 years), of whom all had fully extinguished scotopic and photopic responses
280 (Table 1).

281 Full-field ERG examination data were available for 35/68 (51.5%) CORD patients. Most
282 commonly, an isolated cone dysfunction was seen in 17/35 (48.6%) patients, at a median age

283 of 33.3 years (IQR: 30.3-38.3 years), and a cone-rod pattern in 14/35 (40.0%) patients at a
284 median age of 35.7 years (IQR: 30.2-46.9 years). Four patients (11.4%) had a normal ERG at
285 a median age of 19 years (range: 5-34 years). Goldmann visual fields were available for 12/68
286 (16.6%) CORD patients. In 9/12 patients (75.0%), the Goldmann visual field showed a central
287 scotoma, in 2/12 (16.6%) a ring scotoma, and no visual field defects in 1/12 (8.3%) patients.

288 **Genetic characteristics and genotype-phenotype correlations**

289 In the LCA patients, a total of 14 different *GUCY2D* variants were identified. Ten (71.4%) of
290 these variants were missense mutations, 3 (31.4%) were nonsense mutations, and 1 (7.1%)
291 was a frameshift mutation (Supplemental Table 2 and 3, available at
292 www.opthalmologyretina.org). Two of the LCA patients were siblings (patient 27 and 28),
293 while the remaining 12 patients were isolated cases. The most common variant in these
294 patients was c.1694T>C (p.(Phe565Ser)), which was found in 4 patients, with 3 being
295 homozygous and 1 patient being compound heterozygous. Four patients were compound
296 heterozygous for c.2302C>T (p.(Arg768Trp)) with different variants on the other allele. The
297 two siblings mentioned before both had a homozygous c.2773G>T (p.(Glu925*)) variant,
298 which has not been reported before. Other novel variants in this cohort were the c.518dup
299 (p.(Tyr173*)), c.2861_2862del (p.(Leu954fs*16)), and c.2939A>C (p.(His980Pro)) variants.
300 The c.2620G>A (p.(Glu874Lys)) found in patient 12 has been reported earlier reported in a
301 case of autosomal recessive CORD, but to our knowledge not in LCA yet.²⁰

302 In CORD, 3 different variants were found, all of which involved codon 838 (Supplemental
303 Table 3 and 4, available at www.opthalmologyretina.org). The most common variant was
304 c.2513G>A (p.(Arg838His)), which was found in 37/68 (54.4%) patients from 16 different
305 families. This included one large multigenerational family of 15 affected members from the
306 Netherlands. The c.2512C>T (p.(Arg838Cys)) variant was present in 30/68 (44.1%) patients
307 from 24 families. The aforementioned variants were both missense variants. One CORD

308 patient (1.5%) had the complex (p.(Glu837_Arg838delinsAspSer)) variant and had an
309 atypical phenotype with extensive atrophy in the entire inferior pole (Fig 4A-C). The BCVA
310 at baseline and the rate of BCVA decline did not differ between patients with the c.2513G>A
311 and the c.2512C>T variant (P = 0.625 and P = 0.748, respectively; see Supplemental Fig 2,
312 available at www.opthalmologyretina.org).

313

314 **DISCUSSION**

315 This large multicenter retrospective cohort study describes the spectrum of phenotypes,
316 genotypes and natural course of 14 autosomal recessive LCA and 68 autosomal dominant
317 COD patients from 54 presumably unrelated families with disease causing variants in the
318 *GUCY2D* gene.

319 The LCA patients in this cohort showed a severe congenital visual impairment, often in
320 combination with nystagmus and photophobia. This presentation has also been observed in
321 LCA associated with other genes.² However, in contrast to many other LCA-associated genes,
322 the visual acuity, albeit often severely reduced, appeared to remain relatively stable during
323 follow-up in this cohort of *GUCY2D*-associated LCA patients, and only subtle retinal changes
324 were reported on funduscopy. In the 3 LCA patients with SD-OCT imaging of sufficient
325 quality, a relatively intact retinal structure was observed. This is in accordance with earlier
326 studies on *GUCY2D*-associated LCA, in which slight changes of visual acuity and retinal
327 structure were mostly described in patients above 47 years of age.⁴ However, other studies
328 have shown possible slow decrease of foveal outer nuclear layer thickness and decrease of EZ
329 reflectivity in *GUCY2D*-associated LCA.^{21,22} The description of patients of older age and with
330 longer follow-up periods in future studies may be informative to better determine the long-
331 term functional as well as structural natural course of LCA associated with *GUCY2D*.

332 The study by Bouzia et al. also found 6 relatively milder LCA cases, with two patients even
333 having a visual acuity of 20/60.⁴ This was hypothesized to be due to the presence of at least
334 one missense variant in *GUCY2D* exon 2 in these patients, which presumably causes a less
335 severe phenotype.⁴ In our study on the contrary, visual acuity ranged from no light perception
336 to only 20/200, and the only included patient with a missense variant in exon 2 (c.587A>T
337 (p.(Glu196Val)) had a BCVA of 20/400 at an age of 24 years.

338 In CORD patients of this cohort, disease onset occurred in the second decade of life, and
339 showed a gradual decline in visual acuity of 0.022 logMAR per year. At 56 years, there was a
340 50% estimated probability of having severe visual impairment or being blind based on the
341 better-seeing eye. Funduscopy reports and imaging in CORD showed a progressive
342 development of macular atrophy with increasing age, which can also involve the peripapillary
343 area. The majority of *GUCY2D*-associated CORD patients were myopic; some had severe
344 myopia, which is in accordance with earlier studies.^{5,6,10}

345 Eight CORD patients had a hyporeflective space (optical gap) beneath the macula on SD-
346 OCT (Fig 3J) mimicking subretinal fluid. However, this phenomena has been described
347 previously in IRDs, and is hypothesized to not represent primary leakage of fluid, but rather
348 an empty space, as a result of outer photoreceptor tissue loss.²³

349 The chorioretinal atrophy in advanced cases of *GUCY2D*-associated CORD can also resemble
350 end-stage central areolar choroidal dystrophy associated with the *PRPH2* gene, or geographic
351 atrophy found in end-stage atrophic age-related macular degeneration.²⁴⁻²⁶ The resemblance
352 with AMD has also been described in other IRDs, but the absence of drusen and in most cases
353 an early onset around the second decade of life in *GUCY2D*-associated CORD is helpful in
354 differentiating the condition from AMD.²⁶ However, one patient displayed drusenoid
355 hyperautofluorescent dots on FAF and later developed atrophy (Fig. 3D-H), which could
356 complicate differentiation.

357 It is noteworthy that 3 patients, who were screened for CORD at young age due to known
358 affected family members, had an isolated tritan color vision disturbance, without other clear
359 abnormalities or symptoms.¹⁵ This could indicate that the S-cones, which are sensitive to blue
360 light, may be affected first in *GUCY2D*-associated CORD, and tritan color vision defects may
361 be the earliest measurable symptoms. This finding has not only been described earlier in
362 young *GUCY2D*-associated CORD patients, but has also been found in CORD associated
363 with pathologic variants in the *IRXB* gene cluster.^{27,28} The early S-cone dysfunction may be
364 due to the fact that these cones are more vulnerable to light-induced cell damage, which may
365 be exacerbated by an underlying genetic condition.²⁹ Another explanation could be that the
366 area around the foveal center, which contains the majority of S-cones, is affected first in some
367 IRDs.

368 The c.2513G>A (p.(Arg838His)) and c.2512C>T (p.(Arg838Cys)) variants have been by far
369 the most common in *GUCY2D*-associated CORD in the current cohort, which is similar to
370 earlier studies describing 87% of CORD cases to be associated with these variants.^{10,30} A
371 literature review of 132 *GUCY2D*-associated CORD patients reported that the c.2513G>A
372 (p.(Arg838His)) variant may be associated with a more severe phenotype compared to the
373 c.2512C>T (p.(Arg838Cys)) variant, which was not the case in this cohort of 68 patients.¹⁰
374 Considerable phenotypic variability was observed in this study between subjects, even within
375 families carrying the same *GUCY2D* variant. For example, in the earlier described large
376 family with the c.2513G>A (p.(Arg838His)) variant one patient had a BCVA of 20/33 and
377 another a BCVA of 20/285 both at an age of 35 years. This high degree of interindividual
378 variability, even within families, is well-known in other autosomal-dominantly IRDs such as
379 those associated with the *BEST1* and *PRPH2* genes.^{31,32} The large phenotypic variability in
380 autosomal dominant diseases has been attributed to many factors such as genetic modifiers,
381 allelic variation, variable gene expression or environmental factors.³³⁻³⁶ Incomplete

382 penetrance and variable expressivity has also been documented in other *GUCY2D*-associated
383 *CORD* cohorts, but no clear underlying mechanism or combination of factors has been
384 discovered yet.¹³ We observed a high degree of symmetry in BCVA between eyes in *LCA* as
385 well as *CORD* patients, which would support the use of the fellow-eye as an untreated control
386 eye in future trials. Furthermore, our data suggest that there may be a relatively large window
387 of opportunity for gene therapy in *GUCY2D-LCA*, since visual acuity and photoreceptor
388 layers on the available imaging seemed to remain relatively stable during follow-up. In
389 *GUCY2D*-associated *CORD* severe visual impairment generally started to occur around the
390 fourth decade of life, which suggests that the optimal window of opportunity for future
391 treatments may lay within the first three to four decades of life. However, some *CORD*
392 patients above this age showed relatively intact photoreceptor layers and visual acuity, which
393 would suggest that older individuals may also be eligible for future therapeutic intervention.
394 An increasingly compromised integrity of the EZ and ELM layers, as well as a decrease in
395 CRT, correlated significantly with a decrease in visual acuity, which has also been found
396 previously for several other retinal dystrophies.^{37,38} This may imply that these structural
397 parameters may be suitable criteria for treatment candidate selection, and may serve as
398 (surrogate) endpoints in future therapeutic trials. However, prospective natural history study
399 may be necessary to validate and possibly further develop these endpoints by possibly also
400 including quantitative measurement of changes in these layers. The retrospective nature of
401 this study is associated with certain inherent limitations, such as variability in available data
402 and in intervals between visits. Especially for the *LCA* patients qualitative sufficient imaging
403 as well as long-term follow-up was limited, and future studies with more long-term follow-up
404 may be needed to better understand the spectrum and natural course of *GUCY2D-LCA*.
405 Furthermore, similar to earlier cohorts only a few different variants have been described for
406 *CORD* patients in the current study, which may not represent the entire phenotypic spectrum

407 for *GUCY2D*-associated *CORD*.^{10,30,39} Nonetheless, we have described the currently largest
408 cohort of *GUCY2D*-associated retinal dystrophies and included longitudinal data contrary to
409 most earlier studies. Studies as the current one are not only important to facilitate clinical
410 counseling, but can also aid in choosing the optimal design for future therapeutic as well as
411 prospective natural history studies.

412

413 **References**

- 414 1. Ellingford JM, Barton S, Bhaskar S, et al. Molecular findings from 537 individuals with
415 inherited retinal disease. *J Med Genet.* 2016;53(11):761-767.
- 416 2. Kumaran N, Moore AT, Weleber RG, Michaelides M. Leber congenital
417 amaurosis/early-onset severe retinal dystrophy: clinical features, molecular genetics
418 and therapeutic interventions. *Br J Ophthalmol.* 2017;101(9):1147-1154.
- 419 3. Gill JS, Georgiou M, Kalitzeos A, et al. Progressive cone and cone-rod dystrophies:
420 clinical features, molecular genetics and prospects for therapy. *Br J Ophthalmol.*
421 2019;103(5):711-720.
- 422 4. Bouzia Z, Georgiou M, Hull S, et al. *GUCY2D*-associated Leber congenital amaurosis: a
423 retrospective natural history study in preparation for trials of novel therapies. *Am J*
424 *Ophthalmol.* 2020;210:59-70.
- 425 5. Downes SM, Payne AM, Kelsell RE, et al. Autosomal dominant cone-rod dystrophy
426 with mutations in the guanylate cyclase 2D gene encoding retinal guanylate cyclase-
427 1. *Arch Ophthalmol.* 2001;119(11):1667-1673.
- 428 6. Smith M, Whittock N, Searle A, et al. Phenotype of autosomal dominant cone-rod
429 dystrophy due to the R838C mutation of the *GUCY2D* gene encoding retinal
430 guanylate cyclase-1. *Eye (Lond).* 2007;21(9):1220-1225.
- 431 7. Wimberg H, Lev D, Yosovich K, et al. Photoreceptor guanylate cyclase (*GUCY2D*)
432 mutations cause retinal dystrophies by severe malfunction of Ca(2+)-dependent
433 cyclic GMP synthesis. *Front Mol Neurosci.* 2018;11:348.
- 434 8. Boye SL, Peterson JJ, Choudhury S, et al. Gene therapy fully restores vision to the all-
435 cone *Nrl(-/-) Gucy2e(-/-)* mouse model of Leber congenital amaurosis-1. *Hum Gene*
436 *Ther.* 2015;26(9):575-592.
- 437 9. Jacobson SG, Cideciyan AV, Ho AC, et al. Safety and improved efficacy signals
438 following gene therapy in childhood blindness caused by *GUCY2D* mutations.
439 *iScience.* 2021;24(5):102409.
- 440 10. Sun Z, Wu S, Zhu T, et al. Variants at codon 838 in the *GUCY2D* gene result in
441 different phenotypes of cone rod dystrophy. *Ophthalmic Genet.* 2020;41(6):548-555.
- 442 11. McCullough KT, Boye SL, Fajardo D, et al. Somatic gene editing of *GUCY2D* by AAV-
443 CRISPR/Cas9 alters retinal structure and function in mouse and macaque. *Hum Gene*
444 *Ther.* 2019;30(5):571-589.

- 445 12. van Huet RAC, Oomen CJ, Plomp AS, et al. The RD5000 database: facilitating clinical,
446 genetic, and therapeutic studies on inherited retinal diseases. *Invest Ophthalmol Vis*
447 *Sci.* 2014;55(11):7355-7360.
- 448 13. Udar N, Yelchits S, Chalukya M, et al. Identification of GUCY2D gene mutations in
449 CORD5 families and evidence of incomplete penetrance. *Hum Mutat.*
450 2003;21(2):170-171.
- 451 14. Mukherjee R, Robson AG, Holder GE, et al. A detailed phenotypic description of
452 autosomal dominant cone dystrophy due to a de novo mutation in the GUCY2D gene.
453 *Eye (Lond).* 2014;28(4):481-487.
- 454 15. Went LN, van Schooneveld MJ, Oosterhuis JA. Late onset dominant cone dystrophy
455 with early blue cone involvement. *J Med Genet.* 1992;29(5):295-298.
- 456 16. R Core Team. R: A language and environment for statistical computing. Vienna,
457 Austria: R Foundation for Statistical Computing. <https://www.R-project.org/>; 2020;
458 accessed Januari 12, 2020.
- 459 17. Putter H, Fiocco M, Geskus RB. Tutorial in biostatistics: competing risks and multi-
460 state models. *Stat Med.* 2007;26(11):2389-2430.
- 461 18. Ying GS, Maguire MG, Glynn R, Rosner B. Tutorial on biostatistics: statistical analysis
462 for correlated binary eye data. *Ophthalmic Epidemiol.* 2018;25(1):1-12.
- 463 19. Csaky KG, Richman EA, Ferris FL, III. Report from the NEI/FDA Ophthalmic Clinical
464 Trial Design and Endpoints Symposium. *Invest Ophthalmol Vis Sci.* 2008;49(2):479-
465 489.
- 466 20. Liu X, Fujinami K, Kuniyoshi K, et al. Clinical and genetic characteristics of 15 affected
467 patients from 12 Japanese families with GUCY2D-associated retinal disorder. *Transl*
468 *Vis Sci Technol.* 2020;9(6):2.
- 469 21. Jacobson SG, Cideciyan AV, Sumaroka A, et al. Defining outcomes for clinical trials of
470 Leber congenital amaurosis caused by GUCY2D mutations. *Am J Ophthalmol.*
471 2017;177:44-57.
- 472 22. Jacobson SG, Cideciyan AV, Sumaroka A, et al. Leber congenital amaurosis due to
473 GUCY2D mutations: longitudinal analysis of retinal structure and visual function. *Int J*
474 *Mol Sci.* 2021;22(4).
- 475 23. van Dijk EHC, Boon CJF. Serous business: delineating the broad spectrum of diseases
476 with subretinal fluid in the macula. *Prog Retin Eye Res.* 2021(84):100955.
- 477 24. Boon CJ, Klevering BJ, Cremers FP, et al. Central areolar choroidal dystrophy.
478 *Ophthalmology.* 2009;116(4):771-782, 782.e771.
- 479 25. Smailhodzic D, Fleckenstein M, Theelen T, et al. Central areolar choroidal dystrophy
480 (CACD) and age-related macular degeneration (AMD): differentiating characteristics
481 in multimodal imaging. *Invest Ophthalmol Vis Sci.* 2011;52(12):8908-8918.
- 482 26. Saksens NTM, Fleckenstein M, Schmitz-Valckenberg S, et al. Macular dystrophies
483 mimicking age-related macular degeneration. *Prog Retin Eye Res.* 2014;39:23-57.
- 484 27. Gregory-Evans K, Kelsell RE, Gregory-Evans CY, et al. Autosomal dominant cone-rod
485 retinal dystrophy (CORD6) from heterozygous mutation of GUCY2D, which encodes
486 retinal guanylate cyclase. *Ophthalmology.* 2000;107(1):55-61.
- 487 28. Kohl S, Llavona P, Sauer A, et al. A duplication on chromosome 16q12 affecting the
488 IRXB gene cluster is associated with autosomal dominant cone dystrophy with early
489 tritanopic color vision defect. *Hum Mol Genet.* 2021;30(13):1218-1229.
- 490 29. Haverkamp S, Wässle H, Duebel J, et al. The primordial, blue-cone color system of the
491 mouse retina. *J Neurosci.* 2005;25(22):5438-5445.

- 492 30. Yi Z, Sun W, Xiao X, et al. Novel variants in GUCY2D causing retinopathy and the
493 genotype-phenotype correlation. *Exp Eye Res.* 2021;208:108637.
- 494 31. Boon CJF, Klevering BJ, Leroy BP, et al. The spectrum of ocular phenotypes caused by
495 mutations in the BEST1 gene. *Prog Retin Eye Res.* 2009;28(3):187-205.
- 496 32. Boon CJ, den Hollander AI, Hoyng CB, et al. The spectrum of retinal dystrophies
497 caused by mutations in the peripherin/RDS gene. *Prog Retin Eye Res.* 2008;27(2):213-
498 235.
- 499 33. Green DJ, Sallah SR, Ellingford JM, et al. Variability in gene expression is associated
500 with incomplete penetrance in inherited eye disorders. *Genes (Basel).* 2020;11(2).
- 501 34. Cooper DN, Krawczak M, Polychronakos C, et al. Where genotype is not predictive of
502 phenotype: towards an understanding of the molecular basis of reduced penetrance
503 in human inherited disease. *Hum Genet.* 2013;132(10):1077-1130.
- 504 35. Scheetz TE, Kim KY, Swiderski RE, et al. Regulation of gene expression in the
505 mammalian eye and its relevance to eye disease. *Proc Natl Acad Sci U S A.*
506 2006;103(39):14429-14434.
- 507 36. Gui B, Slone J, Huang T. Perspective: is random monoallelic expression a contributor
508 to phenotypic variability of autosomal dominant disorders? *Front Genet.* 2017;8:191.
- 509 37. Nguyen XT, Talib M, van Cauwenbergh C, et al. Clinical characteristics and natural
510 history of RHO-associated retinitis pigmentosa: a long-term follow-up study. *Retina.*
511 2021;41(1):213-223.
- 512 38. Tee JLL, Yang Y, Kalitzeos A, et al. Natural history study of retinal structure,
513 progression, and symmetry using ellipsoid zone metrics in RPGR-associated
514 retinopathy. *Am J Ophthalmol.* 2019;198:111-123.
- 515 39. Kitiratschky VB, Wilke R, Renner AB, et al. Mutation analysis identifies GUCY2D as the
516 major gene responsible for autosomal dominant progressive cone degeneration.
517 *Invest Ophthalmol Vis Sci.* 2008;49(11):5015-5023.
- 518

519 **Legends Figures**

520 **Figure 1.** Evolution of visual acuity in autosomal dominant cone-rod dystrophy associated
521 with *GUCY2D*. **A**, Plot of linear mixed effects model using the cross-sectional and
522 longitudinal best-corrected visual acuity (BCVA) measurements of the both eyes to predict
523 the average evolution of BCVA with increasing age. In the entire population of *GUCY2D*-
524 *CORD*, a significant annual decline of 0.022 logMAR ($P < 0.001$) was found. **B**, Graph
525 displaying the disease progression estimated by a multistate model in the better-seeing eye.
526 The curves represent the probabilities of having mild visual impairment ($20/67 \leq BCVA <$
527 $20/40$), moderate visual impairment ($20/200 \leq BCVA < 20/67$), severe visual impairment
528 ($20/400 \leq BCVA < 20/200$), and blindness ($BCVA < 20/400$). The distances between the lines
529 indicate the probability of being in a certain category of visual impairment at each age. The
530 distance between: 1) the 0% mark and the green line represents the probability of having no
531 significant visual impairment; 2) between the green and blue line represents the probability of
532 having mild visual impairment; 3) between the blue and yellow line represents the probability
533 of having moderate visual impairment; 4) between the yellow and red line represents severe
534 visual impairment; 5) between the red line and 100% mark represents the probability of being
535 blind, for each individual age. At an age of 40 years the multistate model estimated that
536 *GUCY2D-CORD* patients have a probability of 21.8% to have no significant visual
537 impairment, 5.5% to have mild visual impairment, 41.1% to have moderate visual
538 impairment, 12.4% to have severe visual impairment, and 19.2% to be blind (for further
539 specification of all probabilities at different ages see Supplemental Table 1, available at
540 www.ophtalmologyretina.org). BCVA, best corrected visual acuity; FC, finger counting;
541 HM, hand movements; logMAR, logarithm of the minimum angle of resolution.

542

543 **Figure 2.** Findings on imaging in two patients with *GUCY2D*-associated Leber congenital
544 amaurosis. **A, B, C, D,** Fundus photograph, fundus autofluorescence, near-infrared image and
545 spectral-domain optical coherence tomography (SD-OCT) scan of a 10-year-old patient with
546 heterozygous missense variants in *GUCY2D* (c.2620G>A; p.(Glu874Lys) and c.2939A>C;
547 p.(His980Pro)). On color fundus photography (**A**), mild foveal RPE alterations and on SD-
548 OCT (**D**) an intact retinal anatomy was seen. On fundus autofluorescence (**B**),
549 hyperautofluorescent changes in the fovea were seen, surrounded by a slightly
550 hypoautofluorescent ring with hyperautofluorescent borders. The best-corrected visual acuity
551 (BCVA) was 20/400 in both eyes. **E, F, G, H** Fundus photograph, fundus autofluorescence,
552 near-infrared image and SD-OCT scan of a 28-year-old patient (homozygous c.1694T>C;
553 p.(Phe565Ser) *GUCY2D* variants) with nearly normal appearance on imaging. The BCVA
554 was light perception in both eyes.
555

556 **Figure 3.** Spectrum of findings on imaging in patients with *GUCY2D*-associated cone-rod
557 dystrophy (CORD). **A**, Normal fundus autofluorescence image of a 30-year-old healthy male
558 as reference showing a typical central hypoautofluorescence in the macular area. **B, C**,
559 Fundus autofluorescence image and spectral-domain optical coherence tomography (SD-
560 OCT) scan of a 17-year-old-patient (c.2513C>T; p.(Arg838Cys) variant in *GUCY2D*). On
561 fundus autofluorescence (**B**), an absence of normal central hypoautofluorescence can be seen
562 compared to the healthy reference (**A**). SD-OCT (**C**) showed a continuous external limiting
563 membrane (ELM) and ellipsoid zone (EZ), with possibly mild irregularity of the subfoveal
564 EZ. The visual acuity was 20/33 in the right and 20/32 in the left eye. **D, E, F**, Fundus
565 photograph, fundus autofluorescence image and SD-OCT scan of the left eye of a 14-year-old
566 patient (c.2513C>T; p.(Arg838Cys) variant in *GUCY2D*). The fundus photograph was
567 normal, but an absence of foveal hypoautofluorescence was observed (**E**). On the SD-OCT
568 scan (**F**) the central EZ layer seemed slightly thickened. Visual acuity was 20/80 in both eyes.
569 **G, H, I, J** Fundus photograph, fundus autofluorescence image and SD-OCT scan of the left
570 eye of a 26-year-old patient (c.2513C>T; p.(Arg838Cys) variant in *GUCY2D*) with a
571 relatively normal presentation on the color fundus photograph and fundus autofluorescence
572 image. On SD-OCT (**I**) at the age of 26, slight focal disruption of the EZ was present, with an
573 ELM in the macular area that was largely intact and a best-corrected visual acuity (BCVA) of
574 20/50. Interestingly, one year later this patient developed bilateral, hyporeflective spaces
575 (optical gap) in the central maculae, mimicking subretinal fluid accumulation (**J**). The BCVA
576 dropped to 20/100 in the left eye at this last visit. **K, L, M**, Color fundus photograph, fundus
577 autofluorescence and SD-OCT image of a 28-year-old patient (c.2512C>T; p.(Arg838Cys)
578 variant in *GUCY2D*) showing macular atrophy. The color fundus photograph (**K**) showed
579 atrophic macular mottling, fundus autofluorescence (**L**) showed a small hyperautofluorescent
580 center surrounded by a hypoautofluorescent ring with a hyperautofluorescent border. SD-OCT

581 (M) revealed macular thinning with an absent central EZ and ELM and attenuated outer
582 nuclear layer (BCVA in both eyes: 20/400). N, O, P, Color fundus photograph, fundus
583 autofluorescence and SD-OCT image of the right eye of a 52-year-old patient (c.2513G>A;
584 p.(Arg838His) *GUCY2D* variant) with marked atrophy of the central macula. Fundus
585 photography shows central chorioretinal atrophy (N). This area corresponds to an absence of
586 autofluorescence (O), and a profound atrophy of the central retina on SD-OCT (P). Q, R, S, T
587 Color fundus photograph, fundus autofluorescence and SD-OCT of a 46-year-old patient
588 (c.2512C>T; p.(Arg838Cys) *GUCY2D* variant) with extensive macular, parapapillary and also
589 peripheral atrophy. An absence of autofluorescence can be seen in a relatively large central
590 area and around the optic disc, surrounded by a hyperautofluorescent border (R). Thinning of
591 the retina around the optic disc can also be seen on SD-OCT (S, T). The BCVA of this eye
592 was counting fingers in both eyes.

593 **Figure 4.** Atypical imaging findings in cone-rod dystrophy associated with *GUCY2D* A, B, C
594 Fundus autofluorescence, near-infrared image, and SD-OCT scan of a patient
595 (c.2511_2512delinsCA (p.(Glu837_Arg838delinsAspSer) complex variant) with an atypical
596 *GUCY2D*-CORD phenotype with extensive atrophic changes in the entire inferior pole. The
597 visual acuity was 1.8 logMAR. D, Fundus autofluorescence image of a patient (c.2513G>A
598 p.(Arg838His) *GUCY2D* variant) with drusenoid hyperautofluorescent dots and an optical gap
599 on SD-OCT (F). During follow-up the patient developed macular atrophy (F, G, H).

Table 1. Clinical Characteristics of Patients with *GUCY2D*-Associated Leber Congenital Amaurosis and Cone-Rod Dystrophy

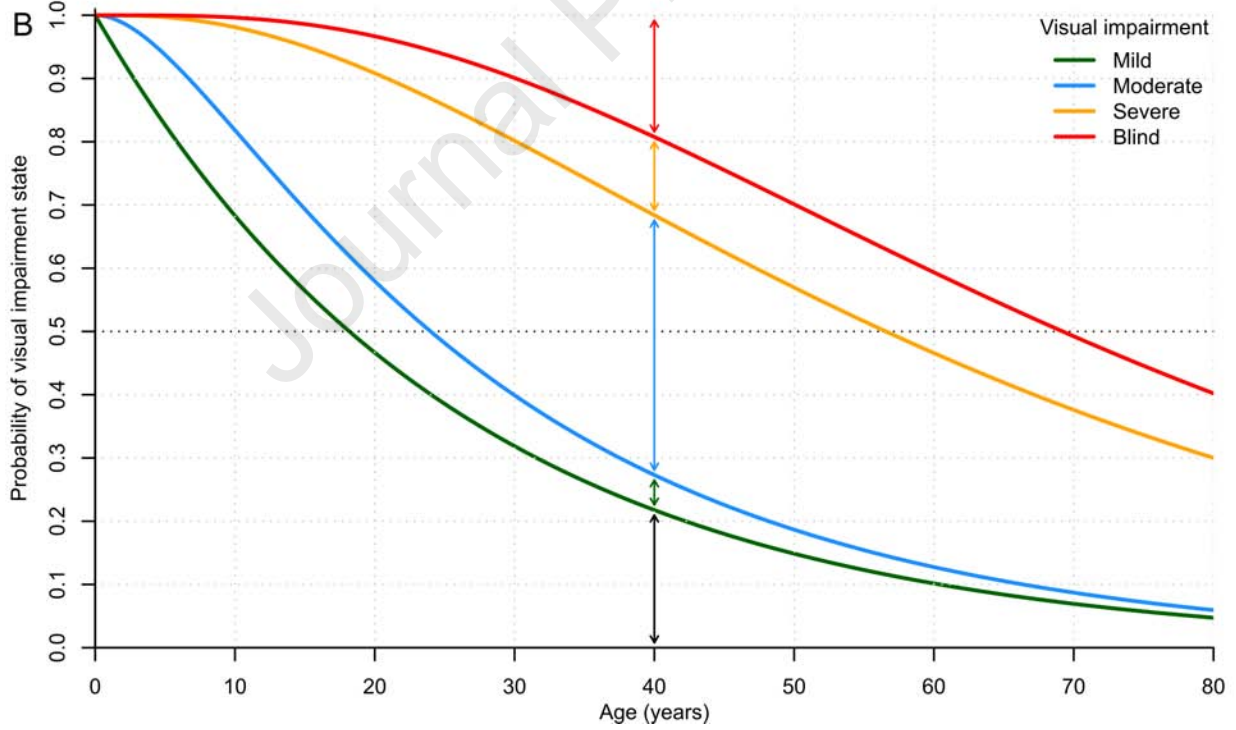
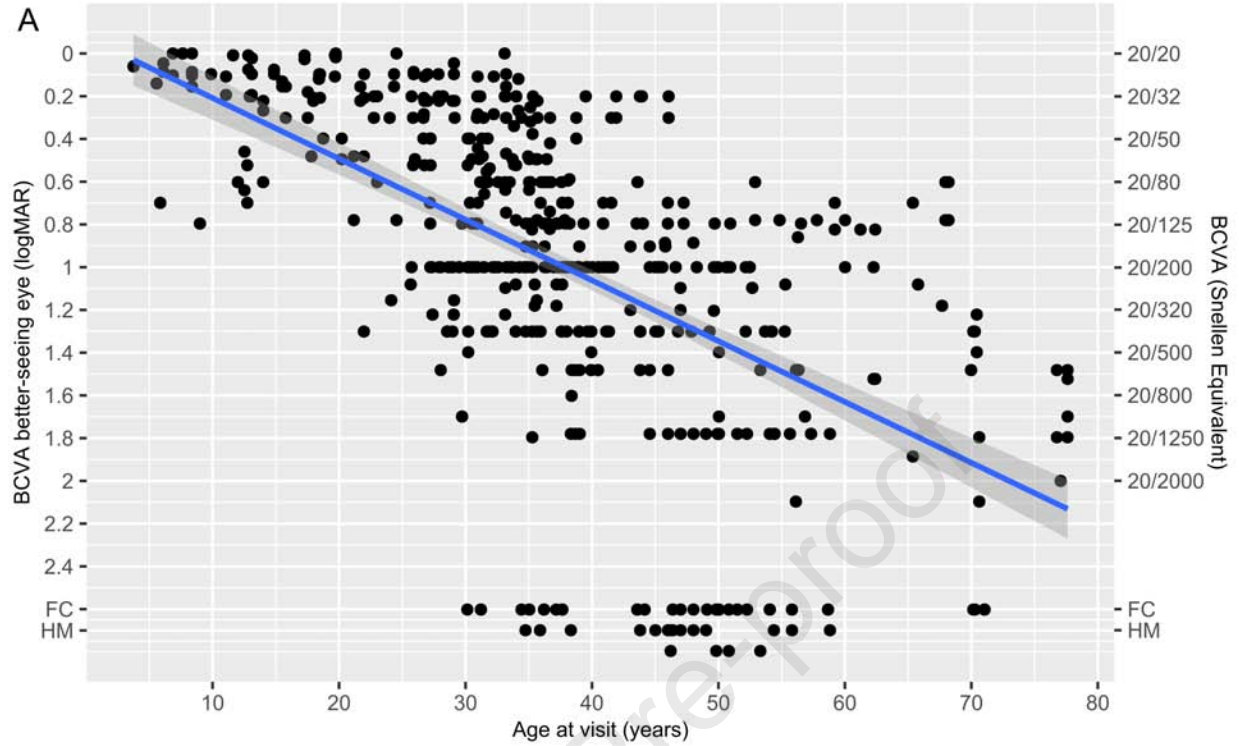
Characteristics	LCA (n = 14)	CORD (n = 68)
Gender		
Male, n (%)	6/14 (43%)	32/68 (47%)
Female, n (%)	8/14 (57%)	36/68 (53%)
Age at onset, n (%) ^b	14/14 (100%)	49/68 (72%)
Median (IQR), years	0.3 (0.0-0.6)	14.7 (10.0-26.5)
Range, years	0.0-2.2	2.0-40.0
Age at last examination		
Mean ± SD, years	13.2 ± 11.3	42.5 ± 16.3
Median (IQR), years	9.9 (7.1-16.4)	40.5 (32.1-54.0)
Range, years	0.6-35.6	9.9-78.4
Number of visits		
Mean ± SD	4.2 ± 2.0	5.3 ± 4.0
Median (IQR)	3.0 (3.0-5.0)	4.0 (3.0-7.0)
Range	2.0-8.0	2.0-21.0
Follow-up time, n (%) ^b	12/14 (86%)	53/68 (78%)
Median follow-up time (IQR), years	5.2 (2.6-8.8)	7.2 (2.2-14.2)
Range, years	0.2-15.9	0.3-77.7
Spherical equivalent refraction, n (%) ^b	6/14 (43%)	35/68 (52%)
Median (IQR), D	2.3 (2.0 to 4.9)	-4.1 (-6.6 to -0.6)
Range, D	1.4 to 9.0	-18.8 to 2.6
High myopia (<-6), n (%)	0/13 (0%)	10/35 (29%)
Moderate myopia (-3D > SER ≥ -6D), n (%)	0/13 (0%)	8/35 (23%)
Mild myopia (-0.75D > SER ≥ -3D), n (%)	0/13 (0%)	6/35 (17%)
SER ≥ -0.75, n (%)	6/6 (100%)	11/35 (31%)
Last available BCVA better-seeing eye, n (%) ^b	12/14 (86%)	67/68 (99%)
Median BCVA, logMAR (IQR)	2.8 (1.4-2.8)	0.9 (0.26-1.3)
Median BCVA, Snellen equivalent (IQR)	LP (LP to 20/500)	20/150 (20/400-20/36)
Last available BCVA worse-seeing eye, n (%) ^b	12/14 (86%)	67/68 (99%)
Median BCVA, logMAR (IQR)	2.8 (2.6-2.8)	1.0 (0.5-1.6)
Median BCVA, Snellen equivalent (IQR)	LP (LP to CF)	20/200 (20/660-20/67)
Recorded symptoms ^a , n (%) ^b	14/14 (100%)	65/68 (96%)
Nystagmus	11/14 (79%)	0/65 (0%)
Photophobia	6/14 (43%)	24/65 (37%)
Nyctalopia	1/14 (7%)	1/65 (2%)
Color vision disturbance	1/14 (7%)	14/65 (22%)
Full-field electroretinogram pattern, n (%) ^b	5/14 (36%)	35/68 (52%)
Scotopic and photopic extinguished	5/5 (100%)	0/35 (0%)
Cone isolated	0/5 (0%)	17/35 (49%)
Cone-rod pattern	0/5 (0%)	14/35 (40%)
Normal	0/5 (0%)	4/35 (11%)

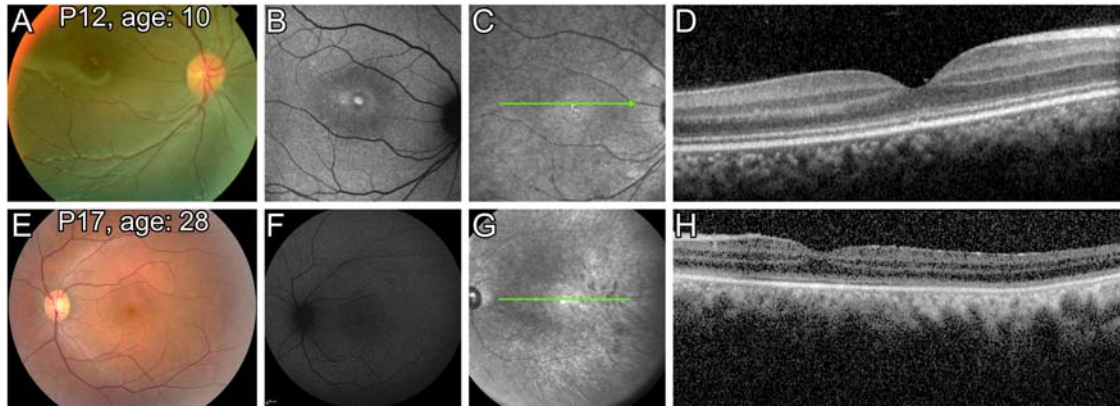
^a Patients could present multiple different symptoms simultaneously; ^b availability of data. BCVA, best-corrected visual acuity; D, diopters; CF, counting fingers; LP, light perception; IQR, interquartile range; logMAR, logarithm of the minimum angle of resolution; RPE, retinal pigment epithelium; SD, standard deviation; SER, spherical equivalent refraction.

Table 2. Imaging Findings in Patients with GUCY2D-Associated Cone-Rod Dystrophy and Leber Congenital Amaurosis at first visit

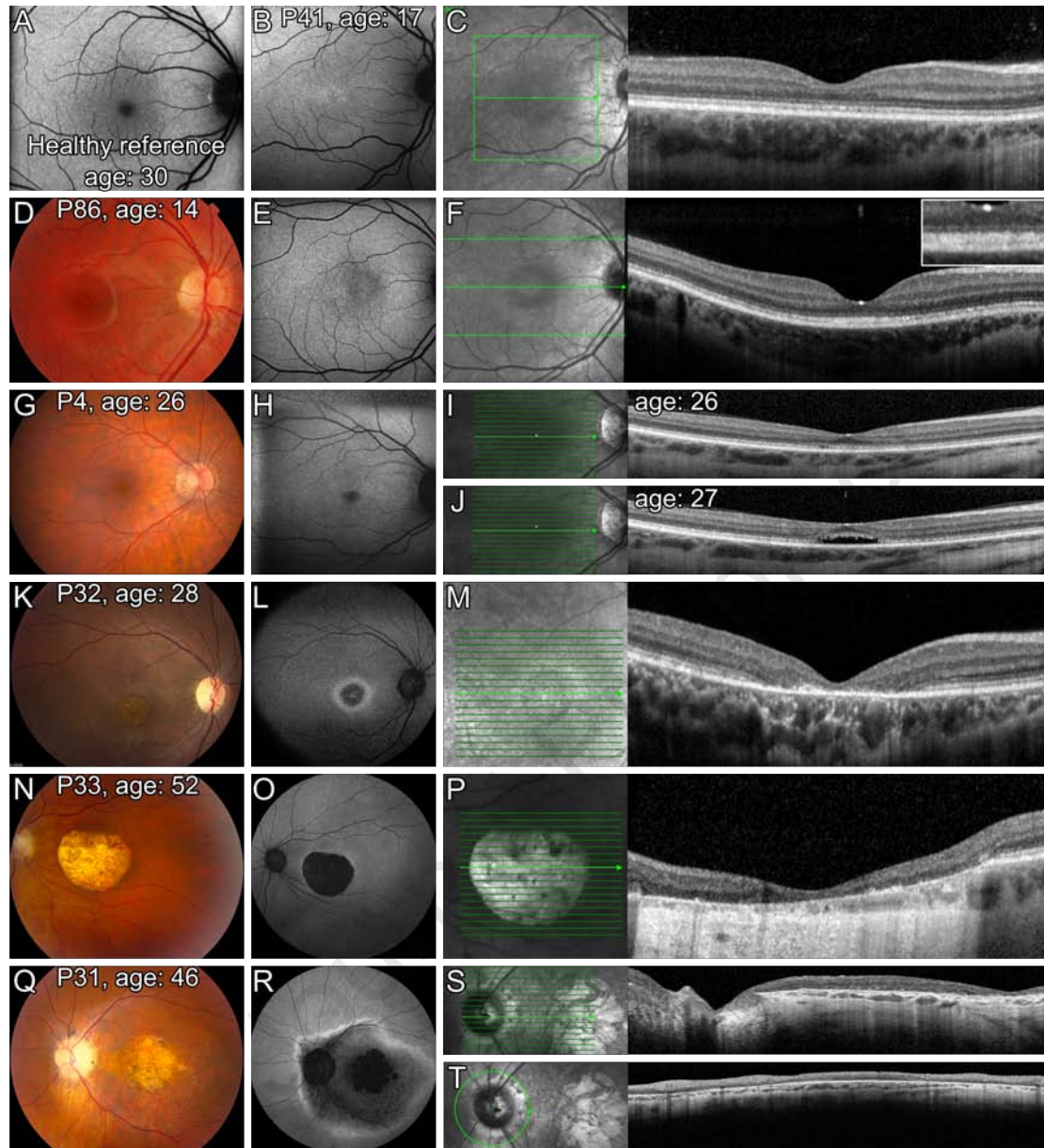
Cone-rod Dystrophy		n (%)	Age (years)
FAF	Increased foveal AF or hyper-AF	16/45 (36%)	5.5-67.9
	Increased foveal AF or hyper-AF with hyper-AF borders	4/45 (9%)	12.9-56.5
	Central granular AF with hyper-AF borders	13/45 (29%)	33.2-65.4
	Central AF absence with hyper-AF borders	6/45 (13%)	36.2-49.6
	Central AF absence without hyper-AF borders	4/45 (9%)	36.2-49.6
	Other FAF pattern	2/45 (4%)	35.7- 54.2
Structural Integrity on SD-OCT			
EZ	Intact	9/47 (19%)	5.6-37.0
	Disrupted	9/47 (19%)	12.5-68.0
	Absent	29/47 (62%)	27.4-70.2
ELM	Intact	18/46 (39%)	5.6-68.0
	Disrupted	4/46 (9%)	12.8-37.0
	Absent	24/46 (52%)	27.4-70.2
Leber Congenital Amaurosis		n (%)	Age (years)
	Normal FAF pattern	1/5 (20%)	15.5
	Increased foveal AF or hyper-AF	2/5 (40%)	9.8-28.9
	Foveal hyper-AF with hyper-AF borders	1/5 (20%)	10.3
	Hyper-AF ring only	1/5 (20%)	28.1
Structural Integrity on SD-OCT			
EZ/ELM	Intact	3/3 (100%)	12.0-28.0

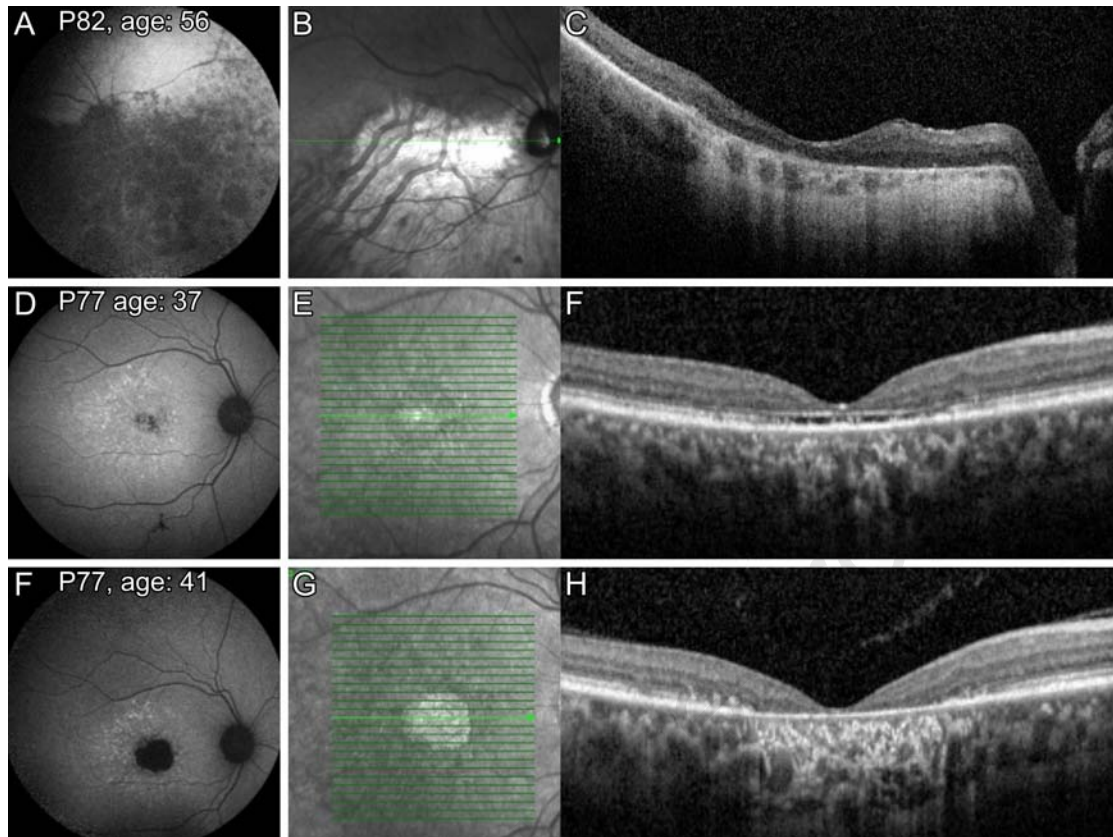
AF, autofluorescence; ELM, external limiting membrane; EZ, ellipsoid zone; FAF, fundus autofluorescence; SD-OCT, spectral-domain optical coherence tomography.





Journal Pre-proof





Journal

Précis

Leber congenital amaurosis and cone-rod dystrophy associated with the *GUCY2D* gene may be promising candidates for future gene therapy due to their natural history and genetic properties.

Journal Pre-proof